Ultra-low threshold deep-ultraviolet generation in hollow-core fiber

MOHAMMED SABBAH[1,*], KERRIANNE HARRINGTON[2], LEAH R. MURPHY[1], CHRISTIAN BRAHMS[1], STEPHANOS YEROLATSITIS[2], JAMES M. STONE[2], TIM A. BIRKS[2], AND JOHN C. TRAVERS[1]

[1] School of Engineering and Physical Sciences, Heriot-Watt University, Edinburgh, United Kingdom
[2] Centre for Photonics and Photonic Materials, Department of Physics, University of Bath, Claverton Down, Bath, BA2 7AY, United Kingdom
[*] m.sabbah@hw.ac.uk

Compiled April 8, 2024

Tunable ultrashort pulses in the ultraviolet spectral region are in great demand for a wide range of applications, including spectroscopy and pump-probe experiments. While laser sources capable of producing such pulses exist, they are typically very complex. Notably, resonant dispersive-wave (RDW) emission has emerged as a simple technique for generating such pulses. However, the required pulse energy used to drive the RDW emission, so far, is mostly at the microjoule level, requiring complicated and expensive pump sources. Here, we present our work in lowering the pump energy threshold for generating tuneable deep-ultraviolet pulses to the level of tens of nanojoules. We fabricated a record small-core anti-resonant fiber with a hollow core-diameter of just 6 µm. When filled with argon, the small mode area enables higher-order soliton propagation and deep-ultraviolet (220 nm to 270 nm) RDW emission from 36 fs pump pulses at 515 nm with the lowest pump energy reported to date. This approach will allow the use of low-cost and compact laser oscillators to drive nonlinear optics in gas-filled fibers for the first time.

http://dx.doi.org/10.1364/ao.XX.XXXXXX

Resonant dispersive-wave (RDW) emission from solitons in gas-filled hollow core fibers is an established technique for generating tunable pulses from the vacuum ultraviolet to the near-infrared (110 to 740 nm) [1–4] with few femtosecond pulse duration [5–7]. During soliton self-compression of the pump pulse along the fiber, its spectrum broadens until it overlaps with a phase-matched wavelength in the normal dispersion region [8, 9], allowing an efficient transfer of energy to a linearly propagating RDW. In hollow-core fibers, the phase-matched RDW wavelength can be tuned simply by changing the pressure of the filling gas.

Ultraviolet RDW emission has already been applied to ultrafast spectroscopy experiments [10–12] but has not yet been transferred to applications outside of advanced laser laboratories due to its dependence, so far, on high-energy ultrafast laser systems. This arises from the use of gas-filled hollow fibers with a core-diameter ranging from ∼25 µm up to ∼450 µm [1, 13]. Even the lower end of this range usually requires the pump energy to be at the µJ level, requiring amplified laser systems. Recently, the use of a much smaller core size enabled the use of less than 150 nJ pump energy from a chirped-pulse amplification Ti:sapphire laser system to achieve ultraviolet RDW emission [14]. While energy up-scaling of ultraviolet RDW emission in hollow capillaries is well understood [3], the fundamental limits of energy down-scaling of this process in antiresonant fibers have not yet been established.

In this work, we experimentally demonstrate the generation of deep ultraviolet RDWs using an argon-filled antiresonant hollow core fiber with a core diameter of just 6 µm pumped with tens of nanojoules of pulse energy. This is nearly an order-of-magnitude lower energy than previous work and paves the way for driving deep ultraviolet pulse generation with low-cost and compact laser oscillators, opening up new application areas. In addition, we show that the dynamics can be scaled up in power by tuning the repetition rate.

It is well established that when down-scaling energy for nonlinear optics, the geometry must be down-scaled to maintain the peak intensity [15]. We must therefore use smaller-core hollow fibres to lower the energy threshold of RDW emission. In that case, pumping at shorter wavelengths is also an advantage due to much lower propagation losses [16, 17]. Furthermore, we have noticed that pumping with a shorter wavelength, closer to the deep ultraviolet region we wish to target, reduces undesired ionization [18, 19], as it reduces the required broadening and hence the required pump intensity. Therefore, in this paper, we first explore this observation in more detail through numerical simulations, considering the fundamental (1030 nm) and the second-harmonic (515 nm) of our pump laser. The model we use is based on the unidirectional pulse propagation equation [20]. It includes the full dispersion, Kerr effect, photoionization, and plasma dynamics. The code used in this work is available at [21].

To facilitate a fair comparison between pump wavelengths, we aim to generate a similar RDW energy and wavelength (240 nm), pumped with the same pump pulse duration (35 fs full-width half-maximum). We adjust the gas filling pressure in all cases to obtain similar phase-matching for all pump wavelengths, core sizes, and the pump energy to obtain similar deep ultraviolet energy. For the 6 µm core-diameter case, the core is filled with argon at 188 bar for the fundamental pump and 44 bar for the second-harmonic.

Fig. 1(a) shows the simulated deep ultraviolet RDW spectrum generated by the two different pump wavelengths. The required input pulse energy is 24 nJ for the 515 nm pump and more than double at 56 nJ for the 1030 nm pump. In both cases, the energy in the deep ultraviolet region is 2.38 nJ. Fig. 1(b) shows the intensity profile corresponding to

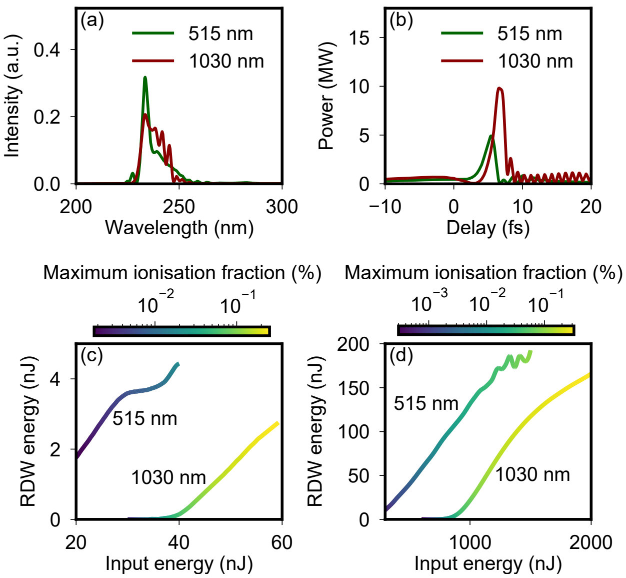

Fig. 1. Simulation results for generating deep ultraviolet RDWs when pumping at 1030 nm or 515 nm. The input pulse duration used for both simulations is 35 fs and the fiber diameter is 6 µm filled with argon at 188 bar for the 1030 nm pump case, and 44 bar for the 515 nm pump case (tuned to obtain RDW phase-matching at around 240 nm). (a) Deep ultraviolet spectrum and (b) intensity profile at the maximum ionization percentage. (c) The change in generated ultraviolet RDW energy as the input energy is changed for both pump wavelengths in a 6 µm core-diameter fiber with pressure tuned to obtain RDW phase-matching at around 240 nm. The line coloring indicates the change in the maximum ionisation fraction for each input energy. Note that we are presenting the ionisation fraction as a percentage of the total gas density for each case separately. (d) Same as (c) but for a 30 µm core-diameter fiber.

the highest ionisation fraction for both scenarios. The intensity for the 1030 nm case is more than twice that of the 515 nm case. Consequently, the ionization fraction for the 515 nm pump is 0.0045%, while for the 1030 nm pump, it is significantly higher at 0.227%, despite the fact that shorter wavelengths tend to ionize more strongly (note that we make use of the ionisation model due to Permolov *et al.* [22]). Consequently, the absolute density is much higher for the 1030 nm case as the pressure is 4 times higher than the 515 nm case. The high ionization fraction observed in the 1030 nm case can cause an inter-pulse effect at high repetition rates, as discussed in previous studies [19, 23, 24].

Fig. 1(c) illustrates how the output ultraviolet RDW energy varies with the input energy for either pump wavelength, using the above parameters. The coloring of the lines indicates the maximum ionisation fraction. Notably, the same ultraviolet energy can be achieved when pumping at 515 nm with less than half the energy required for the 1030 nm pump. Furthermore, the ionisation fraction is more than one order of magnitude lower for the same ultraviolet energy in the 515 nm case. The above discussion also holds for a larger core-diameter, as can be seen in Fig. 1(d). For a large core diameter, a lighter noble gas at higher pressure can be used to reduce the effect of ionization. This becomes impractical for smaller core diameters. For example, when pumping a 30 µm core-diameter fiber at 1030 nm, to obtain phase-matching to a RDW centered at 240 nm, the 8.6 bar of argon can be replaced by 185 bar of helium. However, when pumping a 6 µm core-diameter fiber at 1030 nm, the the required 188 bar of argon would need to be replaced with an unfeasibly high helium pressure in order

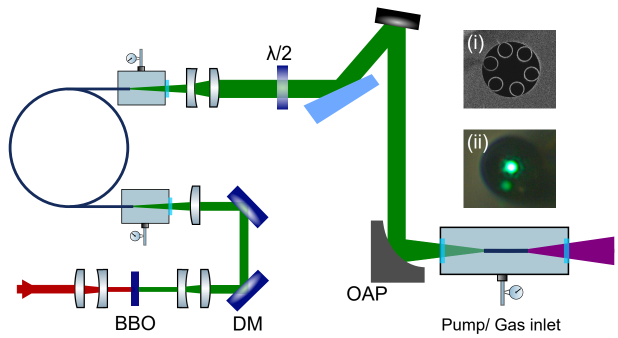

Fig. 2. Experimental setup. DM: dichroic mirror, $\lambda/2$: half-waveplate, OAP: off-axis parabolic mirror. (i) Scanning electron micrograph of the 6 µm fiber. (ii) Optical micrograph of the fiber output face, showing the output beam's near field (the weak spot below the fiber core is a reflection from the microscope lens).

to phase-match the same 240 nm RDW.

An additional requirement for efficient deep ultraviolet RDW generation is that the pulse duration needs to be a few tens of femtoseconds or less [25]. Therefore, when starting from ytterbium-based laser systems a pre-compression stage is usually required [26].

Based on these considerations, we chose to pump the small-core antiresonant fibre with compressed pulses at 515 nm, the frequency-doubled output of our 220 fs [full width at half-maximum (FWHM)] ytterbium laser system operating at 1030 nm. The experimental setup is shown in Fig. 2. To compress the frequency-doubled pulses we used a soliton self-compression stage using an additional nodeless single-ring antiresonant fiber with a core-diameter of 15.5 µm and a length of 4 m. The fiber is coiled in a 30 cm diameter circle and is filled with helium in a negative gradient configuration with the input at 12 bar and the output in vacuum. We found that the polarization state was preserved at the output of the fiber. We characterized the output pulses from the compressor stage using an all-reflective second-harmonic generation (SHG) frequency-resolved optical gating (FROG) setup. The nonlinear medium used is a 10 µm thick beta barium borate crystal cut for type-I

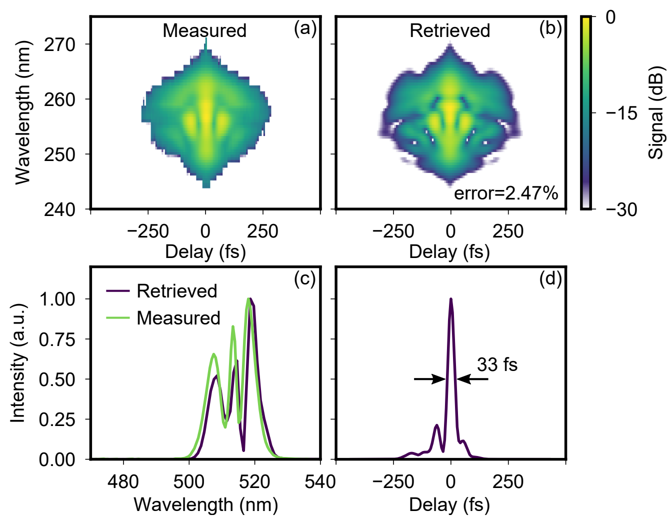

Fig. 3. (a) Measured and (b) retrieved SHG FROG traces on a logarithmic color scale when driving the compression stage with 1 µJ. (c) Measured and retrieved spectrum. (d) Temporal profile of the retrieved pulse.

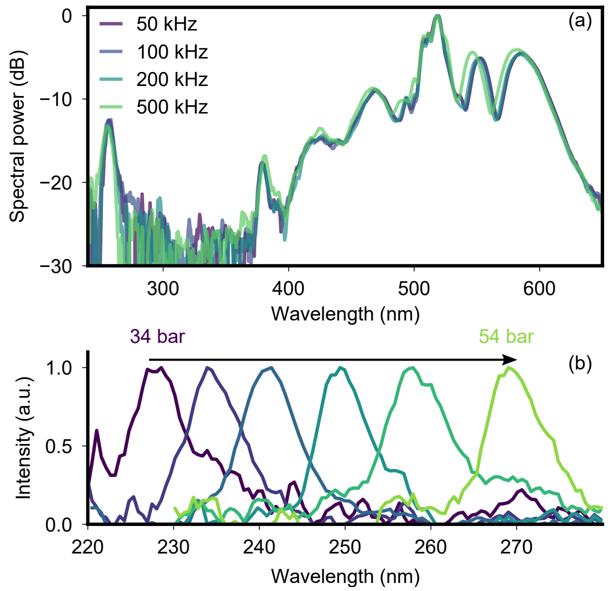

Fig. 4. (a) Experimental spectrum at different repetition rates obtained using ∼20 nJ transmitted energy and 48 bar Ar-filled 6 µm core-diameter fiber. (b) Experimental spectrum of the RDW obtained by tuning the Ar pressure from 34 to 54 bar at 50 kHz.

phase-matching ($\theta = 50.1°$).

Fig. 3(a) and (b) show the measured and retrieved FROG traces for 1 µJ input pulse energy. Fig. 3(d) shows the retrieved pulse temporal profile with 33 fs FWHM. Due to the negative gradient configuration, the pulse acquires extra anomalous dispersion (around $-500\,\mathrm{fs}^2$). This is desired to pre-compensate for the air path and the optics in the beam path to the RDW generation fiber. By numerically propagating the pulse through the optics and air path, the pulse FWHM at the input of the ultraviolet generation stage fiber is 36 fs.

Fig. 2(i) shows a cross-section of the 6 µm fiber used for RDW generation. The fiber is fabricated using the usual stack-and-draw technique [27] and then tapered to its final dimensions [28, 29]. The wall thickness of the fiber resonators is ∼ 148 nm. The fiber is 5 cm long and is placed inside a gas cell with optical access provided by two 6.3 mm thick uncoated fused silica windows. To couple into the 6 µm core-diameter fiber while maintaining the pulse temporal and spatial quality, a 25.4 mm aperture off-axis parabolic mirror (OAP) is used. The OAP avoids the additional chromatic and geometrical dispersion that would be caused by a lens. Note that geometrical dispersion cannot be easily compensated for [30]. Fig. 2(ii) shows a micrograph of the fiber output facet, showing the near-field of the output beam. The energy coupled to the second fiber is controlled and strongly attenuated by a half-wave plate and reflection from a glass wedge.

Fig. 4(a) shows the normalized experimental output spectra on a logarithmic scale when filling the fiber with 48 bar argon and pumping at different repetition rates, ranging from 50 kHz up to 500 kHz. The results presented use ∼20 nJ of transmitted pump energy (measured when the fiber is at vacuum). The deep ultraviolet RDW is emitted at 257 nm with a total efficiency of 1.7% of the transmitted power at 50 kHz. The ultraviolet efficiency slightly drops with increasing repetition rate, to around 1.2% at 500 kHz. This could be due to the heating of the gas and/or the glass due to imperfect coupling at the fiber input face. The power of the RDW is extracted from the spectral power density measured with an integrating sphere and a fiber-coupled spectrometer which has been calibrated as a system on an absolute scale using NIST-traceable lamps.

Fig. 4(b) shows the normalized spectra of the generated deep ultraviolet RDW as the argon pressure is tuned from 34 bar to 54 bar. Over this pressure range, the central wavelength of the RDW can be continuously tuned across the deep ultraviolet transmission window of the fiber from below 230 nm up to 270 nm.

In principle, further down-scaling of the pump energy required for deep-ultraviolet RDW emission is possible by further reducing the core-size. This approach becomes increasingly challenging, due to the increased leakage losses of small core fibres (proportional to the inverse sixth power of the core radius $1/a^6$ [17, 31]), and due to the complications of coupling short (∼ 30 fs) visible pulses into the small core while avoiding chromatic and geometrical dispersion.

In conclusion, we have numerically investigated the effect of pump wavelength on ionisation fraction during deep ultraviolet RDW generation. We have shown that a pump wavelength closer to the RDW wavelength reduces the amount of ionization, making it possible to scale up the repetition rate. Moreover, deep ultraviolet RDW generation has been experimentally achieved using just tens of nanojoules of pump energy. This is the lowest energy used to generate deep ultraviolet pulses in a gas-filled hollow-core fiber to date and paves the way towards ultra-compact and low-cost deep ultraviolet sources for applications outside of advanced laser laboratories. It may also enable direct conversion of laser oscillators to the deep ultraviolet, providing a promising route to deep ultraviolet frequency combs.

Funding. This work was funded by the United Kingdom's Engineering and Physical Sciences Research Council: Grant agreement EP/T020903/1; and by the Institution of Engineering and Technology (IET) through the IET A F Harvey Engineering Research Prize. C.B. acknowledges support from the Royal Academy of Engineering through Research Fellowship No. RF/202122/21/133.

Disclosures. The authors declare no conflicts of interest.

REFERENCES

1. N. Y. Joly, J. Nold, W. Chang, P. Hölzer, A. Nazarkin, G. K. L. Wong, F. Biancalana, and P. S. J. Russell, Phys. Rev. Lett. **106**, 203901 (2011).
2. A. Ermolov, K. F. Mak, M. H. Frosz, J. C. Travers, and P. S. J. Russell, Phys. Rev. A **92**, 033821 (2015).
3. J. C. Travers, T. F. Grigorova, C. Brahms, and F. Belli, Nat. Photonics **13**, 547 (2019).
4. C. Brahms, F. Belli, and J. C. Travers, Phys. Rev. Res. **2**, 043037 (2020).
5. A. Ermolov, H. Valtna-Lukner, J. Travers, and P. S. Russell, Opt. Lett. **41**, 5535 (2016).
6. C. Brahms, D. R. Austin, F. Tani, A. S. Johnson, D. Garratt, J. C. Travers, J. W. G. Tisch, P. S. Russell, and J. P. Marangos, Opt. Lett. **44**, 731 (2019).
7. M. Reduzzi, M. Pini, L. Mai, F. Cappenberg, L. Colaizzi, F. Vismarra, A. Crego, M. Lucchini, C. Brahms, J. C. Travers, R. Borrego-Varillas, and M. Nisoli, Opt. Express **31**, 26854 (2023).
8. M. Erkintalo, Y. Q. Xu, S. G. Murdoch, J. M. Dudley, and G. Genty, Phys. Rev. Lett. **109**, 223904 (2012).
9. K. F. Mak, J. C. Travers, P. Hölzer, N. Y. Joly, and P. S. J. Russell, Opt. Express **21**, 10942 (2013).
10. H. Bromberger, A. Ermolov, F. Belli, H. Liu, F. Calegari, M. Chávez-Cervantes, M. T. Li, C. T. Lin, A. Abdolvand, P. S. J. Russell, A. Cavalleri, J. C. Travers, and I. Gierz, Appl. Phys. Lett. **107** (2015).
11. N. Kotsina, F. Belli, S.-f. Gao, Y.-y. Wang, P. Wang, J. C. Travers, and D. Townsend, The journal physical chemistry letters **10**, 715 (2019).
12. N. Kotsina, C. Brahms, S. Jackson, J. C. Travers, and D. Townsend, Chem. Sci. **13**, 9586 (2022).
13. C. Brahms, F. Belli, and J. C. Travers, Phys. Rev. Res. **2**, 043037 (2020).
14. D. Xiong, J. Luo, M. R. A. Hassan, X. Wu, and W. Chang, Photon. Res. **9**, 590 (2021).

15. C. M. Heyl, H. Coudert-Alteirac, M. Miranda, M. Louisy, K. Kovacs, V. Tosa, E. Balogh, K. Varjú, A. L'Huillier, A. Couairon, and C. L. Arnold, Optica **3**, 75 (2016).
16. E. A. J. Marcatili and R. A. Schmeltzer, The Bell Syst. Tech. J. **43**, 1783 (1964).
17. E. N. Fokoua, S. A. Mousavi, G. T. Jasion, D. J. Richardson, and F. Poletti, Adv. Opt. Photon. **15**, 1 (2023).
18. J. R. Koehler, F. Köttig, D. Schade, P. S. J. Russell, and F. Tani, Opt. Express **29**, 4842 (2021).
19. M. Sabbah, F. Belli, C. Brahms, F. Yu, J. Knight, and J. C. Travers, Opt. Lett. **48**, 2277 (2023).
20. M. Kolesik and J. V. Moloney, Phys. Rev. E **70**, 036604 (2004).
21. C. Brahms and J. C. Travers, "Luna.jl: A flexible nonlinear optical pulse propagator," https://github.com/LupoLab/Luna.jl (2021).
22. A. M. Perelomov, V. S. Popov, and M. V. Terent 'ev, Sov. Phys. JETP **23**, 1393 (1966).
23. J. R. Koehler, F. Köttig, B. M. Trabold, F. Tani, and P. S. Russell, Phys. Rev. Appl. **10**, 064020 (2018).
24. D. Schade, F. Köttig, J. R. Koehler, M. H. Frosz, P. S. J. Russell, and F. Tani, Opt. Express **29**, 19147 (2021).
25. J. C. Travers, W. Chang, J. Nold, N. Y. Joly, and P. S. J. Russell, J. Opt. Soc. Am. B **28**, A11 (2011).
26. K. F. Mak, M. Seidel, O. Pronin, M. H. Frosz, A. Abdolvand, V. Pervak, A. Apolonski, F. Krausz, J. C. Travers, and P. S. J. Russell, Opt. Lett. **40**, 1238 (2015).
27. G. T. Jasion, J. R. Hayes, N. V. Wheeler, Y. Chen, T. D. Bradley, D. J. Richardson, and F. Poletti, Opt. Express **27**, 20567 (2019).
28. T. A. Birks, "Photonic bandgap fibres," in *2008 34th European Conference on Optical Communication,* (2008), pp. 1–30.
29. R. Pennetta, M. T. Enders, M. H. Frosz, F. Tani, and P. S. Russell, APL Photonics **4**, 056105 (2019).
30. M. Kempe and W. Rudolph, Opt. Lett. **18**, 137 (1993).
31. D. Bird, Opt. Express **25**, 23215 (2017).

FULL REFERENCES

1. N. Y. Joly, J. Nold, W. Chang, P. Hölzer, A. Nazarkin, G. K. L. Wong, F. Biancalana, and P. S. J. Russell, “Bright spatially coherent wavelength-tunable deep-uv laser source using an ar-filled photonic crystal fiber,” Phys. Rev. Lett. **106**, 203901 (2011).
2. A. Ermolov, K. F. Mak, M. H. Frosz, J. C. Travers, and P. S. J. Russell, “Supercontinuum generation in the vacuum ultraviolet through dispersive-wave and soliton-plasma interaction in a noble-gas-filled hollow-core photonic crystal fiber,” Phys. Rev. A **92**, 033821 (2015).
3. J. C. Travers, T. F. Grigorova, C. Brahms, and F. Belli, “High-energy pulse self-compression and ultraviolet generation through soliton dynamics in hollow capillary fibres,” Nat. Photonics **13**, 547–554 (2019).
4. C. Brahms, F. Belli, and J. C. Travers, “Infrared attosecond field transients and uv to ir few-femtosecond pulses generated by high-energy soliton self-compression,” Phys. Rev. Res. **2**, 043037 (2020).
5. A. Ermolov, H. Valtna-Lukner, J. Travers, and P. S. Russell, “Characterization of few-fs deep-uv dispersive waves by ultra-broadband transient-grating xfrog,” Opt. Lett. **41**, 5535–5538 (2016).
6. C. Brahms, D. R. Austin, F. Tani, A. S. Johnson, D. Garratt, J. C. Travers, J. W. G. Tisch, P. S. Russell, and J. P. Marangos, “Direct characterization of tuneable few-femtosecond dispersive-wave pulses in the deep uv,” Opt. Lett. **44**, 731–734 (2019).
7. M. Reduzzi, M. Pini, L. Mai, F. Cappenberg, L. Colaizzi, F. Vismarra, A. Crego, M. Lucchini, C. Brahms, J. C. Travers, R. Borrego-Varillas, and M. Nisoli, “Direct temporal characterization of sub-3-fs deep uv pulses generated by resonant dispersive wave emission,” Opt. Express **31**, 26854–26864 (2023).
8. M. Erkintalo, Y. Q. Xu, S. G. Murdoch, J. M. Dudley, and G. Genty, “Cascaded phase matching and nonlinear symmetry breaking in fiber frequency combs,” Phys. Rev. Lett. **109**, 223904 (2012).
9. K. F. Mak, J. C. Travers, P. Hölzer, N. Y. Joly, and P. S. J. Russell, “Tunable vacuum-uv to visible ultrafast pulse source based on gas-filled kagome-pcf,” Opt. Express **21**, 10942–10953 (2013).
10. H. Bromberger, A. Ermolov, F. Belli, H. Liu, F. Calegari, M. Chávez-Cervantes, M. T. Li, C. T. Lin, A. Abdolvand, P. S. J. Russell, A. Cavalleri, J. C. Travers, and I. Gierz, “Angle-resolved photoemission spectroscopy with 9-eV photon-energy pulses generated in a gas-filled hollow-core photonic crystal fiber,” Appl. Phys. Lett. **107** (2015).
11. N. Kotsina, F. Belli, S.-f. Gao, Y.-y. Wang, P. Wang, J. C. Travers, and D. Townsend, “Ultrafast molecular spectroscopy using a hollow-core photonic crystal fiber light source,” The journal physical chemistry letters **10**, 715–720 (2019).
12. N. Kotsina, C. Brahms, S. Jackson, J. C. Travers, and D. Townsend, “Spectroscopic application of few-femtosecond deep-ultraviolet laser pulses from resonant dispersive wave emission in a hollow capillary fibre,” Chem. Sci. **13**, 9586–9594 (2022).
13. C. Brahms, F. Belli, and J. C. Travers, “Infrared attosecond field transients and uv to ir few-femtosecond pulses generated by high-energy soliton self-compression,” Phys. Rev. Res. **2**, 043037 (2020).
14. D. Xiong, J. Luo, M. R. A. Hassan, X. Wu, and W. Chang, “Low-energy-threshold deep-ultraviolet generation in a small-mode-area hollow-core fiber,” Photon. Res. **9**, 590–595 (2021).
15. C. M. Heyl, H. Coudert-Alteirac, M. Miranda, M. Louisy, K. Kovacs, V. Tosa, E. Balogh, K. Varjú, A. L’Huillier, A. Couairon, and C. L. Arnold, “Scale-invariant nonlinear optics in gases,” Optica **3**, 75–81 (2016).
16. E. A. J. Marcatili and R. A. Schmeltzer, “Hollow metallic and dielectric waveguides for long distance optical transmission and lasers,” The Bell Syst. Tech. J. **43**, 1783–1809 (1964).
17. E. N. Fokoua, S. A. Mousavi, G. T. Jasion, D. J. Richardson, and F. Poletti, “Loss in hollow-core optical fibers: mechanisms, scaling rules, and limits,” Adv. Opt. Photon. **15**, 1–85 (2023).
18. J. R. Koehler, F. Köttig, D. Schade, P. S. J. Russell, and F. Tani, “Post-recombination effects in confined gases photoionized at megahertz repetition rates,” Opt. Express **29**, 4842–4857 (2021).
19. M. Sabbah, F. Belli, C. Brahms, F. Yu, J. Knight, and J. C. Travers, “Generation and characterization of frequency tunable sub-15-fs pulses in a gas-filled hollow-core fiber pumped by a yb:kgw laser,” Opt. Lett. **48**, 2277–2280 (2023).
20. M. Kolesik and J. V. Moloney, “Nonlinear optical pulse propagation simulation: From maxwell’s to unidirectional equations,” Phys. Rev. E **70**, 036604 (2004).
21. C. Brahms and J. C. Travers, “Luna.jl: A flexible nonlinear optical pulse propagator,” https://github.com/LupoLab/Luna.jl (2021).
22. A. M. Perelomov, V. S. Popov, and M. V. Terent ’ev, “Ionization of atoms in an alternating electric field,” Sov. Phys. JETP **23**, 1393–1409 (1966).
23. J. R. Koehler, F. Köttig, B. M. Trabold, F. Tani, and P. S. Russell, “Long-lived refractive-index changes induced by femtosecond ionization in gas-filled single-ring photonic-crystal fibers,” Phys. Rev. Appl. **10**, 064020 (2018).
24. D. Schade, F. Köttig, J. R. Koehler, M. H. Frosz, P. S. J. Russell, and F. Tani, “Scaling rules for high quality soliton self-compression in hollow-core fibers,” Opt. Express **29**, 19147–19158 (2021).
25. J. C. Travers, W. Chang, J. Nold, N. Y. Joly, and P. S. J. Russell, “Ultrafast nonlinear optics in gas-filled hollow-core photonic crystal fibers [invited],” J. Opt. Soc. Am. B **28**, A11–A26 (2011).
26. K. F. Mak, M. Seidel, O. Pronin, M. H. Frosz, A. Abdolvand, V. Pervak, A. Apolonski, F. Krausz, J. C. Travers, and P. S. J. Russell, “Compressing μj-level pulses from 250 fs to sub-10 fs at 38-mhz repetition rate using two gas-filled hollow-core photonic crystal fiber stages,” Opt. Lett. **40**, 1238–1241 (2015).
27. G. T. Jasion, J. R. Hayes, N. V. Wheeler, Y. Chen, T. D. Bradley, D. J. Richardson, and F. Poletti, “Fabrication of tubular anti-resonant hollow core fibers: modelling, draw dynamics and process optimization,” Opt. Express **27**, 20567–20582 (2019).
28. T. A. Birks, “Photonic bandgap fibres,” in *2008 34th European Conference on Optical Communication,* (2008), pp. 1–30.
29. R. Pennetta, M. T. Enders, M. H. Frosz, F. Tani, and P. S. Russell, “Fabrication and non-destructive characterization of tapered single-ring hollow-core photonic crystal fiber,” APL Photonics **4**, 056105 (2019).
30. M. Kempe and W. Rudolph, “Impact of chromatic and spherical aberration on the focusing of ultrashort light pulses by lenses,” Opt. Lett. **18**, 137–139 (1993).
31. D. Bird, “Attenuation of model hollow-core, anti-resonant fibres,” Opt. Express **25**, 23215–23237 (2017).